

# Synthesis, antitumor evaluation and DNA photocleaving activity of novel methylthiazonaphthalimides with aminoalkyl side chains

Zhigang Li,<sup>a</sup> Qing Yang<sup>b</sup> and Xuhong Qian<sup>a,c,\*</sup>

<sup>a</sup>State Key Lab. of Fine Chemicals, Dalian University of Technology, PO Box 158, Zhongshan Road, Dalian 116012, China

<sup>b</sup>Department of Bioscience and Biotechnology, Dalian University of Technology, Dalian 116012, China

<sup>c</sup>Shanghai Key Lab. of Chemical Biology, School of Pharmacy, East China University of Science and Technology, Shanghai 200237, China

Received 1 February 2005; revised 5 April 2005; accepted 8 April 2005

Available online 3 May 2005

**Abstract**—A series of methylthiazonaphthalimides was synthesized and quantitatively evaluated as efficient DNA intercalators, anti-tumor agents and DNA photocleavers. **A**<sub>1</sub> showed both efficient antitumor activities against cell lines of A549 and P388 with IC<sub>50</sub> of 82.8 and 31 nM, respectively. **A**<sub>3</sub> was the strongest antitumor agent against A549 with the IC<sub>50</sub> of 20.8 nM. **A**<sub>2</sub>, the most efficient DNA intercalator, was found to be the strongest DNA photocleaver via superoxide anion. An explanation was given for the discord between antitumor and DNA photocleaving activities.  
© 2005 Elsevier Ltd. All rights reserved.

Naphthalimides constitute an important class of drugs in anticancer therapy which have shown high antitumor activities upon a variety of murine and human tumor cells.<sup>1,2</sup> They are characterized by the presence of a planar chromophore, generally a tri- or tetracyclic ring system and one or two flexible basic side chains. Novel naphthalimides with an extra aromatic ring fused to the naphthalimide skeletons have been reported, especially by Braña and co-workers.<sup>3</sup> Most active mononaphthalimides showed cytotoxic activities in the order of 10<sup>−6</sup>–10<sup>−7</sup> M. The presence of a larger aromatic ring can improve the affinity of the intercalator for the DNA molecule, consequently to a greater cytotoxic potency than the parent compound amonafide (Fig. 1).<sup>3</sup> Also many of such agents have shown the capability of generating various reactive intermediates that resulted in DNA photocleavage.<sup>4</sup>

Our previous study has demonstrated that the presence of sulfur rather than its oxo-counterpart promoted the DNA intercalating and photocleaving ability.<sup>5</sup> On the basis of introducing a fused aromatic ring or sulfur atom to the naphthalimide skeleton to result in higher antitu-

mor and/or DNA photocleaving activities, we synthesized a new series of thio-heterocyclic fused naphthalimides, **A**<sub>1–4</sub>, and evaluated their DNA intercalating property, antitumor and DNA photocleaving activities (Fig. 1). The thiazole ring, being appeared in several known anticancer antibiotics<sup>6</sup> or DNA photocleaver,<sup>4c</sup> has been angularly fused to the naphthalimide skeleton. *N,N*-Dimethyl aminoethyl group and similar analogues, commonly applied in anticancer drugs, were incorporated into the parent structure not only to increase the affinity with DNA<sup>1–5</sup> but also to elucidate the influence of them on biological activities.

These methylthiazonaphthalimides were synthesized from 4-bromo-3-nitro-1,8-naphthalic anhydride<sup>7</sup> as

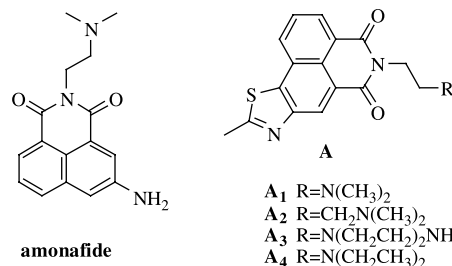
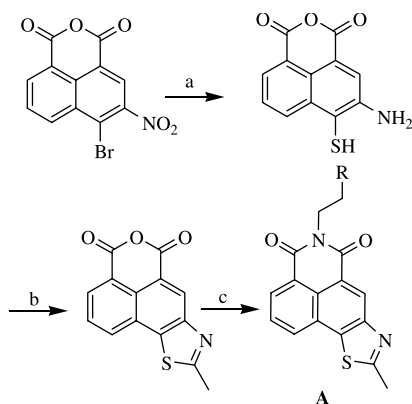


**Figure 1.** Structures of amonafide and novel methylthiazonaphthalimides.

**Keywords:** Methylthiazonaphthalimide; Antitumor; Intercalate; Photocleaver.

\*Corresponding author. Tel.: +86 411 83673466; fax: +86 411 83673488; e-mail addresses: xhqian@dlut.edu.cn; xhqian@ecust.edu.cn



**Scheme 1.** Synthesis of methylthiazonaphthalimides. Reagents and conditions: (a)  $\text{Na}_2\text{S}_2$ ,  $\text{H}_2\text{O}$ , 8 h; (b) acetaldehyde,  $\text{AcOH}$ ,  $\text{N}_2$ , reflux 4 h, 65% yield; (c) corresponding amine, ethanol, reflux 3 h.

shown in Scheme 1. 4-Bromo-3-nitro-1,8-naphthalic anhydride was reacted with sodium disulfide in water under reflux for 8 h to obtain the solution of 4-mercapto-3-amino naphthalic anhydride. Due to its instability in air, the reaction mixture was filtrated and dropped into glacial acetic acid containing acetaldehyde immediately, then refluxed for further 4 h to give methylthiazole fused naphthalic anhydride as the most important intermediate. The obtained anhydride was then condensed with corresponding amine in ethanol to form the target product of interest. Structures of all these final products were identified by  $^1\text{H}$  NMR, HRMS, IR.<sup>8</sup>

The aminoalkyl side chains were found to have slight effect on the UV–vis and fluorescent data of **A**<sub>1–4</sub> (Table 1). Their maxim absorptions were around 350 nm with similar intensities around 4.0 (log  $\epsilon$ ). They also had the similar emissions at about 425 nm with weak fluorescent intensities.

The fluorescences of **A**<sub>1–4</sub> were quenched upon addition of Calf thymus DNA. Their Scatchard binding constants<sup>9</sup> (Table 2) were all above  $\sim 10^5 \text{ M}^{-1}$  (Fig. 2), indicating their efficient binding abilities via intercalation by the methylthiazonaphthalimide chromophores. The side chain with three methylene units between dimethyl-amino group and diimide moiety can significantly enhance the affinity of **A**<sub>2</sub> to DNA as shown by the binding order of **A**<sub>2</sub> > **A**<sub>1</sub>  $\approx$  **A**<sub>3</sub>  $\approx$  **A**<sub>4</sub>.

All these methylthiazonaphthalimides were evaluated for their antitumor activities in vitro against cell lines of A549 (human lung cancer cell) and P388 (murine leuk-

**Table 1.** Spectra data of methylthiazonaphthalimides **A**<sub>1–4</sub><sup>a,b</sup>

Compds	UV $\lambda_{\text{max}}$ (lg $\epsilon$ )	FL $\lambda_{\text{max}}$ ( $\Phi$ )
<b>A</b> <sub>1</sub>	351 (4.1)	425 (0.0015)
<b>A</b> <sub>2</sub>	353 (3.92)	423 (0.0028)
<b>A</b> <sub>3</sub>	352 (3.99)	424 (0.0025)
<b>A</b> <sub>4</sub>	353 (3.98)	426 (0.0022)

<sup>a</sup> In absolute ethanol.

<sup>b</sup> With quinine sulfate in sulfuric acid as quantum yield standard ( $\phi = 0.55$ ).

**Table 2.** Cytotoxicities and Scatchard binding constants of compounds **A**<sub>1–4</sub>

Compd	Scatchard binding constants ( $10^5 \text{ M}^{-1}$ )	Cytotoxicity ( $\text{IC}_{50}$ , nM)	
		A549 <sup>a</sup>	P388 <sup>b</sup>
<b>A</b> <sub>1</sub>	2.31	82.8	31
<b>A</b> <sub>2</sub>	6.66	1804	1703
<b>A</b> <sub>3</sub>	2.26	20.8	1127
<b>A</b> <sub>4</sub>	1.66	158	640
Amonafide	NR <sup>c</sup>	1100	200

<sup>a</sup> Cytotoxicity (CTX) against human lung cancer cell (A549) was measured by sulforhodamine B dye-staining method.<sup>10</sup>

<sup>b</sup> CTX against murine leukemia cells (P388) was measured by micro-culture tetrazolium-formazan method.<sup>11</sup>

<sup>c</sup> NR, not reported.

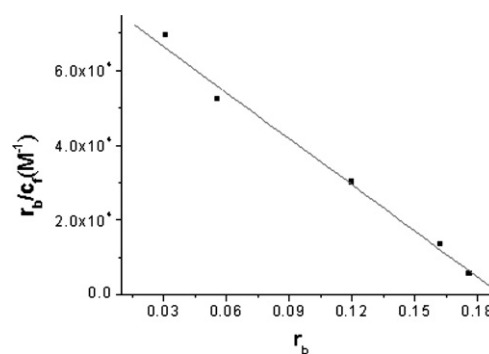


**Figure 2.** Scatchard curve between **A**<sub>2</sub> and Calf thymus DNA.

emia cell), respectively. The results were summarized in Table 2 and compared with the activity of the parent compound of amonafide. The  $\text{IC}_{50}$  represents the drug concentration (nM) required to inhibit the cell growth by 50%.

Obviously, the cytotoxic potency of **A**<sub>1–4</sub> against these two cell lines was highly dependent on structures of the aminoalkyl side chains. **A**<sub>1</sub> showed both efficient antitumor activities against cell lines of A549 and P388 with  $\text{IC}_{50}$  of 82.8 and 31 nM, respectively. Compared to amonafide with  $\text{IC}_{50}$  of 1100 and 200 nM, **A**<sub>1</sub> showed about more than six-fold higher antitumor activity. **A**<sub>3</sub> inhibited the growth of A549 most strongly with the lowest  $\text{IC}_{50}$  of 20.8 nM, indicating that it was nearly 50-fold more cytotoxic against A549 than amonafide. These results are in agreement with our hypothesis that the introduction of a methylthiazole ring to the naphthalimide skeleton would increase the affinity of the chromophore for the target DNA, consequently lead to a greater cytotoxic potency. **A**<sub>1</sub> and **A**<sub>3</sub> showed efficient inhibiting activities even in the order of  $10^{-8} \text{ M}$ , showing their stronger cytotoxicity than most other reported heterocyclic fused mono-naphthalimides, in turn proving the rational design.

These aminoalkyl side chains also significantly influenced the selectivity of these compounds' antitumor activities. **A**<sub>1</sub>, **A**<sub>3</sub>, and **A**<sub>4</sub> were more cytotoxic against A549 than amonafide. However, only **A**<sub>1</sub> was more cytotoxic against P388 than amonafide. **A**<sub>3</sub> is even about

50-fold more cytotoxic against A549 than against P388, reflecting an excellent selectivity for a special human or lung cell type.

The photocleaving activities of **A**<sub>1–4</sub> to supercoiled plasmid pBR322DNA were evaluated by 1% agarose gel electrophoresis. The reaction mixture containing each compound and pBR322DNA was put under a transilluminator (360 nm) at a distance of 20 cm at 0 °C for 3 h under aerobic conditions. The photocleaving efficiency was defined by the ratio of the conversion from supercoiled pBR322DNA (form I) to relaxed circular DNA (form II) and linear DNA (form III). All these new compounds were found to photocleave DNA efficiently from form I to form II at the concentration of 100  $\mu$ M with the order of **A**<sub>2</sub> > **A**<sub>1</sub> > **A**<sub>3</sub> > **A**<sub>4</sub> (Fig. 3a). Under identical conditions, **A**<sub>2</sub> could produce more percentage of form II (77%) and a further damaged form (15% form III), generally the result from double-strand cuts or proximal single-strand cuts on opposite strands (lane 4). Further experiment showed that **A**<sub>2</sub> exhibited detectable cleavage (20% form II) at the concentration of as low as 0.5  $\mu$ M and total cleavage from form I (closed) to form II (nicked) and even form III (linear) at the concentration of 200  $\mu$ M (Fig. 3b), suggesting the cleavage efficiency was concentration dependent. Also **A**<sub>2</sub> photocleaved DNA more efficiently with the elongation of photo-irradiation (Fig. 3c), indicating **A**<sub>2</sub> had good time-controlled photo-bioactivity. No damage was observed in the absence of either compound (lane 2) or light (lane 3) indicating that they were obligate factors for DNA strand scission. In our case, UV light

actually functioned as trigger to initiate the strand scission.

The photocleaving ability order of **A**<sub>1–4</sub> was almost parallel to that of their binding abilities. However, it seemed to be no obvious correlation between DNA photocleaving and antitumor activities. For example, **A**<sub>2</sub> was the most efficient DNA photocleaver while exhibited weakest antitumor activity against A549 and P388. The reason accounting for it probably lies on that: the cytotoxicity of one compound is determined by two conflicting factors including cell membrane crossing ability and DNA binding ability. The side chains could be protonated to different extent under physiological pH due to their different basicity of corresponding nitrogen atoms. The protonation extent significantly affected the ability of the molecule to pass through lipophilic membranes to bind to DNA. Lower degree of protonation is desirable for cell penetration, but higher degree of protonation favored DNA binding. Once these two factors effectively compromise, the higher antitumor potency is possible, such as **A**<sub>1</sub>. High degree of protonation extent may be achieved by **A**<sub>2</sub> which lead to its efficient DNA binding and photocleaving activities. However, the high degree of protonation extent in turn inhibited its cell membrane crossing ability. Poor compromise of these two factors may be achieved by **A**<sub>2</sub> which resulted in its weak antitumor activity in the end. Also, the selective cytotoxicity of **A**<sub>3</sub> was possibly determined by its different membrane crossing ability for different cell lines.

Due to their similar structures, **A**<sub>1–4</sub> may have the same photocleaving mechanism, herein, mechanistic experiments were performed with **A**<sub>2</sub> as an example (Fig. 4) by the addition of histidine (singlet oxygen quencher), dithiothreitol (DTT, superoxide anion scavenger), ethanol (hydroxyl radical scavenger), respectively. As shown in Figure 4, histidine (lane 4) and ethanol (lane 6) had no obvious effect on the photocleavage, indicating that singlet oxygen and hydroxyl radical were not likely to be the cleaving agents. However, the DNA-cleaving activity of **A**<sub>2</sub> decreased greatly in the presence of DTT (lane 5). Thus, we believed superoxide anion was most likely to be involved in the cleavage of plasmid.

In summary, a series of methylthiazonaphthalimides, **A**<sub>1–4</sub>, has been synthesized and evaluated for their

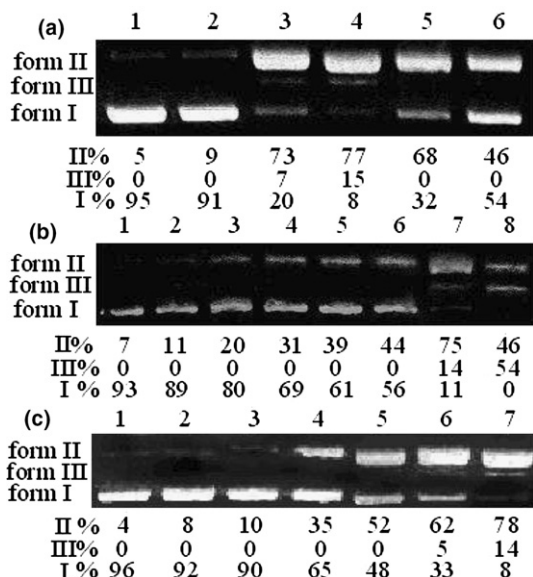


**Figure 3.** Photocleavage of closed supercoiled pBR322DNA (200  $\mu$ M/bp) in the buffer of Tris-HCl (20 mM, pH 7.5). (a) Photocleavage of plasmid pBR322DNA by compounds (100  $\mu$ M) for 3 h. Lane 1, DNA alone (no  $h\nu$ ); lane 2, DNA alone; lanes 3–6, each compound of **A**<sub>1–4</sub> and DNA, respectively. (b) Photocleavage of plasmid pBR322DNA by **A**<sub>2</sub> at various concentrations for 3 h. Lane 1, DNA alone (no  $h\nu$ ); lane 2, DNA alone; lanes 3–8, **A**<sub>2</sub> at concentration of 0.5, 1, 10, 50, 100, 200  $\mu$ M, respectively. (c) Photocleavage of plasmid pBR322DNA by **A**<sub>2</sub> (100  $\mu$ M) at various time intervals. Lane 1, DNA alone (no  $h\nu$ ); lane 2, DNA alone ( $h\nu$  3 h); lanes 3–7, 0, 30, 60, 120, 180 min, respectively.

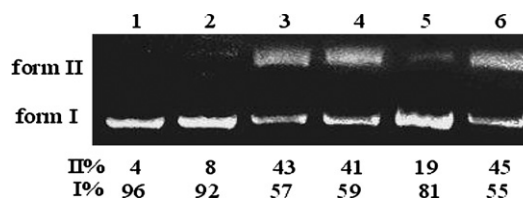


**Figure 4.** Effect of additives on the photocleavage of closed supercoiled pBR322DNA (200  $\mu$ M/bp) by compound **A**<sub>2</sub> (50  $\mu$ M) in the buffer of Tris-HCl (20 mM, pH 7.5) for 3 h. Lane 1, DNA alone (no  $h\nu$ ); lane 2, DNA alone; lanes 3 DNA and compound **A**<sub>2</sub>; lanes 4–6, DNA and compound **A**<sub>2</sub> in the presence of histidine (6 mM), dithiothreitol (DTT, 30 mM), ethanol (1.7 M), respectively.

antitumor and photocleaving activities. The aminoalkyl side chains had different effects on these naphthalimides' antitumor and photocleaving activities. Among these compounds, **A<sub>1</sub>** showed both efficient antitumor activities against A549 and P388. **A<sub>3</sub>** exhibited selective antitumor activity against A549. **A<sub>2</sub>** showed most efficient photocleavage of supercoiled plasmid pBR322DNA. Detectable DNA cleavage of **A<sub>2</sub>** was found at 0.5  $\mu$ M and total cleavage from form I to form II and form III was found at 200  $\mu$ M. Mechanism experiment showed that superoxide anion was involved.

### Acknowledgements

Financial support by the National Key Project for Basic Research (2003CB114400) and under the auspices of National Natural Science Foundation of China is greatly appreciated.

### References and notes

1. Braña, M. F.; Cacho, M.; Gradillas, A.; Pascual-Teresa, B.; Ramos, A. *Curr. Pharm. Des.* **2001**, *7*, 1745–1780.
2. Braña, M. F.; Ramos, A. *Curr. Med. Chem. Anti-cancer Agents.* **2001**, *1*, 237–255.
3. (a) Sami, S. M.; Dorr, R. T.; Alberts, D. S.; Remers, W. A. *J. Med. Chem.* **1993**, *36*, 765–770; (b) Sami, S. M.; Dorr, R. T.; Alberts, D. S.; Solyom, A. M.; Remers, W. A. *J. Med. Chem.* **2000**, *43*, 3067–3073; (c) Braña, M. F.; Cacho, M.; Garcia, M. A.; de Pascual-Teresa, B.; Ramos, A.; Acero, N.; Llinares, F.; Munoz-Mingarro, D.; Abradelo, C.; Rey-Stolle, M. F.; Yuste, M. *J. Med. Chem.* **2002**, *45*, 5813–5816; (d) Braña, M. F.; Cacho, M.; Garcia, M. A.; de Pascual-Teresa, B.; Ramos, A.; Dominguez, M. T.; Pozuelo, J. M.; Abradelo, C.; Rey-Stolle, M. F.; Yuste, M.; Banez-Coronel, M.; Lacal, J. C. *J. Med. Chem.* **2004**, *47*, 1391–1399; (e) Braña, M. F.; Cacho, M.; Ramos, A.; Dominguez, M. T.; Pozuelo, J. M.; Abradelo, C.; Rey-Stolle, M. F.; Yuste, M.; Carrasco, C.; Baily, C. *Org. Biomol. Chem.* **2003**, *1*, 648–654.
4. (a) Li, Y.; Xu, Y.; Qian, X., et al. *Bioorg. Med. Chem. Lett.* **2003**, *13*, 3513–3515; (b) Qian, X.; Li, Y.; Xu, Y., et al. *Bioorg. Med. Chem. Lett.* **2004**, *14*, 2665–2668; (c) Li, Y.; Xu, Y.; Qian, X., et al. *Tetrahedron Lett.* **2004**, *45*, 1247–1251; (d) Xu, Y.; Qu, B.; Qian, X.; Li, Y., et al. *Bioorg. Med. Chem. Lett.* **2005**, *15*, 1139–1142; (e) Li, Z.; Yang, Q.; Qian, X. *Bioorg. Med. Chem. Lett.* **2005**, *15*, 1769–1772.
5. Qian, X.; Huang, T., et al. *J. Chem. Soc., Perkin. Trans. 2* **2000**, 715–718.
6. (a) Quada, J. C.; Levy, M. J.; Hecht, S. M. *J. Am. Chem. Soc.* **1993**, *115*, 12171–12172; (b) Quada, J. C.; Boturnyn, D.; Hecht, S. M. *Bioorg. Med. Chem.* **2001**, *9*, 2303–2314; (c) Thomas, C. J.; McCormick, M. M.; Vialas, C.; Tao, Z. F.; Leitheiser, C. J.; Rishel, M. J.; Wu, X.; Hecht, S. M. *J. Am. Chem. Soc.* **2002**, *124*, 3875–3884; (d) Kuroda, R.; Satoh, H.; Shinomiya, M.; Watarabe, T.; Otsuka, M. *Nucl. Acids Res.* **1995**, *23*, 1524–1530.
7. Yao, W.; Qian, X. *Dyes Pigments* **2001**, *48*, 43–47.
8. **A<sub>1</sub>**: mp 176–177 °C. <sup>1</sup>H NMR (CDCl<sub>3</sub>-d<sub>6</sub>)  $\delta$  (ppm): 2.49 (s, 6H, NCH<sub>3</sub>), 2.84 (t, 2H, NCH<sub>2</sub>), 2.99 (s, 3H, 9-CH<sub>3</sub>), 4.42 (t, *J*<sub>1</sub> 6.8 Hz, *J*<sub>2</sub> 7.2 Hz, 2H, CONCH<sub>2</sub>), 7.83 (t, *J*<sub>1</sub> 7.6 Hz, *J*<sub>2</sub> 8 Hz, 1H, 2-H), 8.31 (d, *J* = 7.6 Hz, 1H, 1-H), 8.64 (d, *J* = 6.4 Hz, 1H, 3-H), 9.08 (s, 1H, 7-H). HRMS (ESI): Calcd for C<sub>18</sub>H<sub>18</sub>N<sub>3</sub>O<sub>2</sub>S (M+H)<sup>+</sup>: 340.1120, Found: 340.1130. IR (KBr): 2920, 2850, 1700, 1660, 1330, 780 cm<sup>-1</sup>. **A<sub>2</sub>**: mp 173–175 °C. <sup>1</sup>H NMR (CDCl<sub>3</sub>-d<sub>6</sub>)  $\delta$  (ppm): 2.82 (m, 2H, NCH<sub>2</sub>), 2.70 (s, 6H, NCH<sub>3</sub>), 2.96 (s, 3H, 9-CH<sub>3</sub>), 3.14 (t, *J*<sub>1</sub> 7.2 Hz, *J*<sub>2</sub> 8.4 Hz, 2 H, CH<sub>2</sub>), 4.13 (t, 2H, CONCH<sub>2</sub>), 7.91 (t, *J*<sub>1</sub> 8 Hz, *J*<sub>2</sub> 7.2 Hz, 1H, 2-H), 8.51 (d, *J*<sub>1</sub> 8.4 Hz, *J*<sub>2</sub> 7.2 Hz, 2H, 1-H, 3-H), 8.768 (s, 1H, 7-H). HRMS (ESI): Calcd for C<sub>19</sub>H<sub>20</sub>N<sub>3</sub>O<sub>2</sub>S (M+H)<sup>+</sup>: 354.1276, Found: 354.1292. IR (KBr): 2920, 2850, 2640, 1700, 1660, 1330, 780 cm<sup>-1</sup>. **A<sub>3</sub>**: mp 168–70 °C. <sup>1</sup>H NMR (CDCl<sub>3</sub>-d<sub>6</sub>)  $\delta$  (ppm): 2.98 (t, 2H, NCH<sub>2</sub> (cycle)), 3.02 (s, 3H, 9-CH<sub>3</sub>), 4.47 (t, *J*<sub>1</sub> 6.8 Hz, *J*<sub>2</sub> 7.6 Hz, 2H, CONCH<sub>2</sub>), 7.84 (t, *J*<sub>1</sub> 7.6 Hz, *J*<sub>2</sub> 8.0 Hz, 1H, 2-H), 8.29 (d, *J* = 8.4 Hz, 1H, 1-H), 8.63 (d, *J* = 7.2 Hz, 1H, 3-H), 9.07 (s, 1H, 7-H). HRMS (ESI): Calcd for C<sub>20</sub>H<sub>21</sub>N<sub>4</sub>O<sub>2</sub>S (M+H)<sup>+</sup>: 381.1385, Found: 381.1377. IR (KBr): 2920, 2850, 2660, 1700, 1660, 1330, 780 cm<sup>-1</sup>. **A<sub>4</sub>**: mp 162–164 °C. <sup>1</sup>H NMR (CDCl<sub>3</sub>-d<sub>6</sub>)  $\delta$  (ppm): 2.49 (s, 10H, NCH<sub>2</sub>CH<sub>3</sub>), 2.84 (t, 2H, NCH<sub>2</sub>), 2.90 (s, 3H, 9-CH<sub>3</sub>), 4.42 (t, *J*<sub>1</sub> 6.8 Hz, *J*<sub>2</sub> 7.2 Hz, 2H, CONCH<sub>2</sub>), 7.83 (t, *J*<sub>1</sub> 7.6 Hz, *J*<sub>2</sub> 8 Hz, 1H, 2-H), 8.31 (d, *J* = 7.6 Hz, 1H, 1-H), 8.64 (d, *J* = 6.4 Hz, 1H, 3-H), 9.09 (s, 1H, 7-H). HRMS (ESI): Calcd for C<sub>20</sub>H<sub>22</sub>N<sub>3</sub>O<sub>2</sub>S (M+H)<sup>+</sup>: 368.1433, Found: 368.1422. IR (KBr): 2920, 2850, 1700, 1660, 1330, 780 cm<sup>-1</sup>.
9. Gupta, M.; Ali, R. *J. Biochem.* **1984**, *95*, 1253–1257.
10. Skehan, P.; Storeny, R.; Scudiero, D.; Monks, A.; McMahon, J.; Vistica, D.; Warren, J. T.; Bokes, H.; Kenney, S.; Boyd, M. R. *J. Natl. Cancer Inst.* **1990**, *82*, 1107.
11. Kuroda, M.; Mimaki, Y.; Sashida, Y.; Hirano, T.; Oka, K.; Dobashi, A.; Li, H.; Harada, N. *Tetrahedron* **1997**, *53*, 11549–11562.